THE ASTROPHYSICAL JOURNAL, 317:102–111, 1987 June 1

1.4 GHz CONTINUUM SOURCES IN THE CANCER CLUSTER

E. E. SALPETER
Center for Radiophysics & Space Research, Cornell University
AND
J. M. DICKEY
Astronomy Department, University of Minnesota
Received 1986 August 4; accepted 1986 November 18

ABSTRACT

We report on 1.4 GHz continuum observations for 11 VLA fields, using the D-configuration, which contain the A group of the Cancer Cluster. Sixteen Zwicky spiral galaxies in the Cancer Cluster were detected, but no ellipticals. We corroborate the finding that spiral galaxies with close companions tend to have enhanced radio emission. Over 200 continuum sources beyond the Cancer Cluster are tabulated. The spectral index (relative to 610 MHz) is given for many of the sources, including some of the Zwicky galaxies. There is a suggestion for a nonuniform number surface-density distribution of the sources, not correlated with the Cancer Cluster. Possible predictions of such nonuniformities, from assumptions on "super-superclusters," are discussed.

Subject headings: galaxies: clustering — galaxies: structure — radio sources: galaxies

I. INTRODUCTION

There is some evidence (Dressel 1981; Hummel 1981*b*) that the statistical properties of the radio continuum emission from galaxies depends on the galaxy's environment. In particular, enhanced emission has been reported (Dressel 1981) from clusters or groups which (*a*) have a moderately high number density of galaxies and (*b*) contain some optically very bright elliptical galaxies. The Cancer Cluster represents an interesting intermediate case: It has been shown (Bothun *et al.* 1983) to consist of a loose, unbound collection of discrete groups which, individually, are bound and moderately compact. In particular, the central group "Cancer A" has (*a*) a moderately high galaxy density, but (*b*) an absence of optically very bright galaxies (and no strong central radio galaxy nor head-tail source). This region has been surveyed at 610 MHz (Perola, Tarenghi, and Valentijn 1980; Valentijn 1980), but not yet at 1.4 GHz. We report here such a continuum 1.4 GHz survey of an area covering 11 VLA (D-array) fields which includes (slightly asymmetrically placed) most of the Cancer A group (and parts of groups B and D).

Optically known cluster galaxies make up only a fairly small fraction of the continuum sources in the surveyed area and we can address some further questions: Unlike the Cancer Cluster, the Hercules Cluster A2151 does contain some very strong radio galaxies, and there is a suggestion (of marginal statistical significance) of an excess of galaxyless continuum sources nearby (Dickey and Salpeter 1984). We shall look for any source excess near the center of Cancer A (although its absence will not cause any big surprise). With most of the continuum emission from background sources, we are able to add a small amount of data to the luminosity function—and a considerable amount of data to the spectral index between 0.61 and 1.4 GHz—for such sources. The area covered by our survey is marginally large enough (~ 2.5 deg^2) to look for nonuniformity in the density of sources: Most observed sources are intrinsically very bright and very rare (and typically at redshifts of order unity); ordinary galaxy clusters and superclusters are therefore not massive enough to contribute significantly to "clumping" of observed sources (when only projected number densities but no redshifts are available). However, the possibility of "super-superclusters" of dimensions (in redshift units) of order 10^4 km s^{-1} ($\Delta z \sim 1/30$) has been suggested by a number of authors recently.

If structures of this size and *large* density contrast occur at $z \sim 0.5$–2, say, then the density of background sources should be "clumpy" on scales of one to a few degrees. Our survey gives one example at the short end of this scale.

II. OBSERVATIONS AND DATA REDUCTION

a) Radio Continuum

The observations were made 1984 September 10 and 23, using the VLA[1] in the closely spaced D-configuration. The standard 20 cm continuum system was used, with two IF's of 50 MHz each centered on 1465 and 1515 MHz, each recording two circular polarizations. Eleven primary beam areas were observed in the Cancer Cluster region. Field centers are indicated on Figure 1. Each field was observed five times, for 10 min each. The phase was calibrated using 0735+178, a nearby point source. Fluxes were calibrated with respect to the primary flux standard 1328+307 (3C 286). The standard NRAO calibration programs were used.

Maps were made on the AIPS system running on the Minnesota Physics and Astronomy VAX which uses an FPS 5105 array processor. Maps were made with 256 × 256 pixels, each 10″ square. The clean beam size was about 44″. Self-calibration (phase only) improved only one or two of the maps, as there are no very strong sources in fields, and only a few stronger than 100 mJy. Typical noise levels were (10.15 to 0.2) mJy rms, leading to detection thresholds from 0.7 to 1.6 mJy. Two fields had significantly worse rms noise, perhaps because of slight gain calibration errors not corrected by self-calibration, or perhaps because of confusion from off the map; they had thresholds of 2.5 and 3.0 mJy.

Each field was studied in detail by hand, and candidate sources were fitted using the AIPs task IMFIT. For the 11

[1] The Very Large Array is operated by the National Radio Astronomy Observatory under contract with the National Science Foundation.

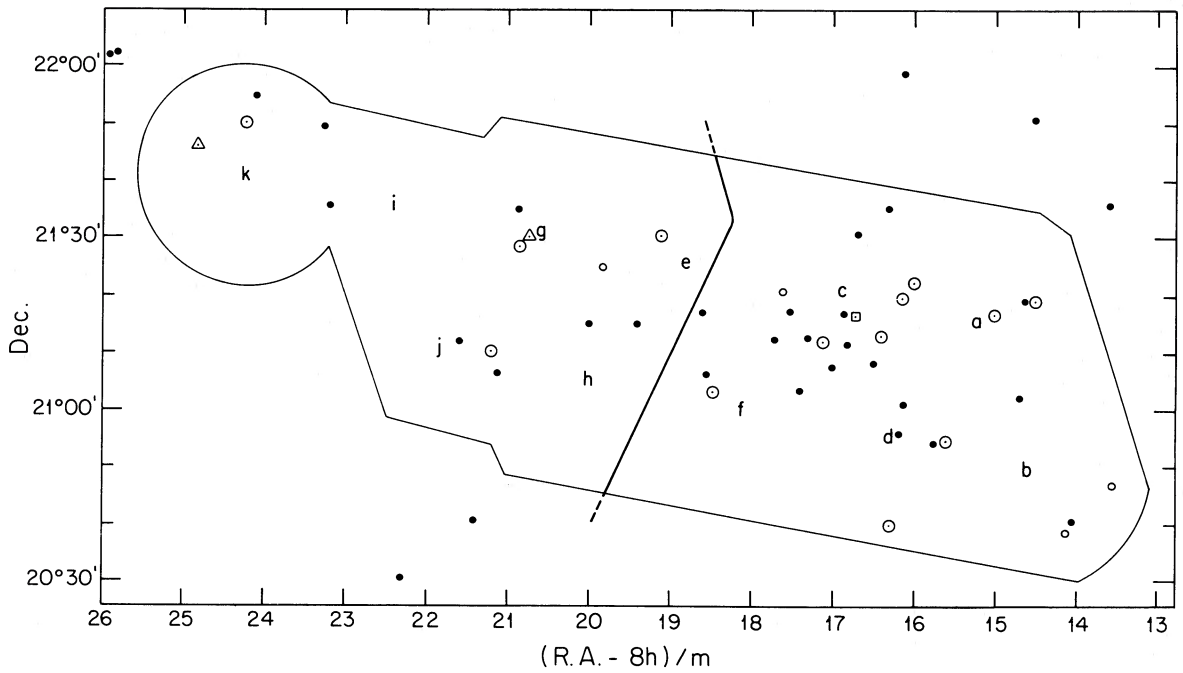

FIG. 1.—Optical galaxies over the 11 VLA fields. The centers of the fields are denoted by small letters. Undetected Zwicky galaxies are denoted by points, detected Zwicky galaxies by large circles surrounding a point (or triangles for 10–20 mJy flux, a square for >20 mJy). The detected non-Zwicky galaxies are denoted by small open circles.

fields we detected a total of 430 continuum sources, counting twice sources in the overlap areas between the field centers. Using these overlap sources we could check the primary beam attenuation factors determined by Napier and Rots (1982) and incorporated in the AIPS task PBCOR. We find that PBCOR does a good job of correcting all overlap sources to the same peak flux, although we find a slight improvement using the function:

$$GF = \exp\left[\left(\frac{z}{18.7}\right)^2 + \left(\frac{z}{28.4}\right)^4\right], \quad (1)$$

where z is the distance from field center in arcminutes and GF is the inverse of the attenuation factor relative to the center of the map. In addition to the primary beam this factor includes the relatively small effect of bandwidth smearing. For measured fluxes near S_{min} the typical flux error is of order $\pm 20\%$.

b) Reduction of the Palomar Observatory Sky Survey Plates

For comparison with optical galaxy properties we have used the Minnesota Automated Plate Scanner to scan the E and O Palomar Observatory Sky Survey Plates of the Cancer Cluster region. The plate scanner and its reduction programs are described by Dickey *et al.* (1987). Following the methods described in that paper we have generated a catalog of galaxies, with center positions fitted relative to SAO stars with rms astrometric errors of 0.″6 and with magnitudes estimated to within 0.5 m relative to the measurements of Schommer, Sullivan, and Bothun (1981). Extending the results for Hercules, we estimate the catalog of galaxies so obtained to be 90% complete for galaxies brighter than $J = 16$, 75% complete down to about $J = 17.5$, and 50% complete to about $J = 18.5$.

The data obtained from the plate scanner were compared with the VLA source list. For each radio source the distance to the nearest optical image was measured. The distribution of these distances shows the expected Poisson shape with a narrow spike superposed centered on zero offset with width about 10″. Since the VLA clean beamwidth was more than 4 times this size we consider this positional accuracy quite good, and we associate as "definitely together" optical images closer than 15″ to a radio source (in Table 3 we include a few doubtful associations with offsets up to 40″).

III. THE SOURCE CATALOG

Centers for the 11 VLA fields are given in Table 1 and Figure 1. The solid closed boundary in Figures 1 and 2 denotes the area inside of which any source with $S_{cor} = S_{map} \times (GF) \gtrsim 6$ mJy should be detected reliably. Table 2 lists all these sources and also quite a few weaker sources inside the area and a number of sources outside the area. Figure 2 plots the positions of all sources with $S_{cor} \geq 10$ mJy. We shall see in § IV

TABLE 1

FIELD CENTER COORDINATES AND MINIMUM RELIABLY MEASURED FLUX S_{min}[a]

Field	R.A. (8h + 1)	Decl.	S_{min} (mJy)
a	15.2m	21°16′	0.7
b	14.6	20°50′	0.8
c	17.0	21°21′	1.2
d	16.4	20°55′	0.9
e	18.8	21°26′	1.2
f	18.2	21°00′	1.2
g	20.6	21°31′	1.0
h	20.0	21°05′	1.6
i	22.4	21°36′	3.0
j	21.8	21°10′	2.5
k	24.2	21°41′	1.2

[a] At a field center.

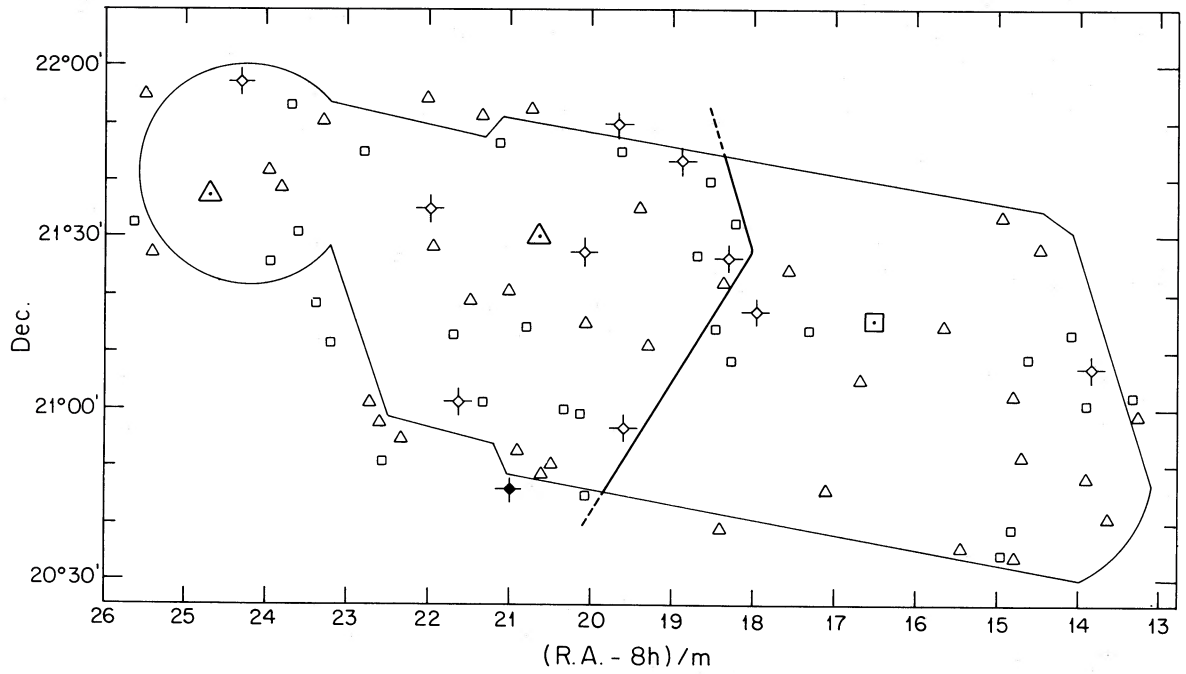

FIG. 2.—Positions for the stronger continuum sources: Triangles for S_{cor} = (10–20) mJy, squares for (20–50) mJy, diamonds for S_{cor} > 50 mJy

that this is an extremely conservative threshold, since a number of very much weaker sources have quite reliable measured positions.

Our source catalog in Table 2 lists the field (or fields) for each source and the gain factor GF (for multiple detections, the smallest value of GF is given and the appropriate field label is underlined). The coordinates of each source center and the corrected "sky flux," $S_{cor} = S_{map} \times (GF)$, are also given in Table 2 (for multiple detections a weighted mean is used). We do not have quantitative rms flux errors but "typical" errors are $\sim \pm 0.25 S_{min} \times (GF)$ with S_{min} given in Table 1.

The AIPS program gives "best fits" to the observed major and minor diameters for all sources and, in principle, one could deconvolve the beam size to give an estimate of the "bare diameters" for the sources themselves. In practice, comparison of multiple detections showed that estimates of the "bare major diameter" were unreliable unless it exceeded $\sim 50''$ (and $S_{map} \sim 6$ mJy). A few "bare" major diameters are given in Table 2 (in brackets, underneath the value for S_{cor}). In no case did we obtain a reliable minor diameter.

As mentioned, Valentijn (1980) has surveyed an overlapping area to much of our 11 VLA fields at 610 MHz with the Westerbork array. Defining the spectral index α between 610 MHz and 1.48 GHz by

$$S_{610}/S_{1480} = (1480/610)^{\alpha}, \quad (2)$$

we give values for α in the last column of Table 2 for all sources detected in both surveys. The frequency distributions of α are given in Figure 3, separately for "low flux" and "high flux" sources (after separating out sources which correspond to optical galaxies in the Zwicky catalog; see § IV). A narrow peak near $\alpha = 0.75$ (already noted by previous authors; see § VI) is seen for both sets of sources. Apart from the intrinsic source properties, the narrowness of the peak for the "low flux" sources shows that *neither* of the two surveys suffer from large flux errors in this flux range. We have no "very high" fluxes in our area, but for our two flux levels the mean values for α are also very similar ($\bar{\alpha} \approx 0.50$ for low flux, ≈ 0.55 for high flux). Previous data, reviewed by Schuch (1983), show a dependence of the α-distribution on flux level, but mainly for very high fluxes and for frequencies above 1 GHz. Our absence of a dependence at lower fluxes and frequencies is not incompatible with these findings. Note that $\bar{\alpha}$ for the Zwicky spirals in the Cancer Cluster is similar to that of the background sources, but there is *no* strong peak near $\alpha = 0.75$.

IV. SOURCES IN OPTICAL GALAXIES

Figure 1 shows (as solid points) the positions of the 41 optical galaxies bright enough ($m_p \leq 15.6$) to be in the Zwicky catalog (Zwicky and Herzog 1963) and inside our survey area. A few Zwicky galaxies just outside this area are also shown. As described in § II we had available optical center coordinates for a large list of galaxies, including all Zwicky galaxies but extending to much fainter apparent magnitudes. Table 3 displays all those sources from Table 2 whose radio coordinates agree, to within about $\pm 20''$ each in both R.A. and decl., with an optical galaxy position. This list includes 16 of the 41 Zwicky galaxies in the survey area, and only four additional sources associated with anonymous, much fainter, galaxies. Bothun *et al.* (1983) give velocities for the Zwicky galaxies and assignments to individual bound groups for the majority; these data are given in column (10) in Table 3 for the 16 detected Zwicky galaxies. Of these, 10 belong to the central Cancer A group ($\bar{V} = 4607$ km s^{-1}), two to Cancer B ($\bar{V} = 6227$ km s^{-1}), one to Cancer D ($\bar{V} = 3506$ km s^{-1}) and three are unassigned (one foreground and two background). The relative assignment

proportions are roughly comparable for the 16 detected and the 25 undetected Zwicky galaxies. The survey area (identical in Figs. 1 and 2) is divided into two equal areas by a curved line (discussed in § V). The dense core of the Cancer A group is concentrated in the right half area, but the fraction of Zwicky galaxies detected at 1.4 GHz does not show any marked preference—10 out of 27 detected in the right half and six out of 14 in the left half. The mean position offsets (optical minus radio) of the 18 sources in Table 3 are $-3\overset{s}{.}9 = -0\overset{s}{.}3$ in R.A. and $-5''.8$ in decl. Note that the offsets for the weakest radio sources are not particularly large.

Hubble types have been assigned for most of the Zwicky galaxies in the Cancer area by various authors (Tifft, Jewsbury, and Sargent 1973; Perola, Tarenghi, and Valentijn 1980; Bothun *et al.* 1985; Giovanelli and Haynes 1985), and these are also given in Table 3. It is a striking fact that none of the detected Zwicky galaxies is E or S0. Four of the detected galaxies in Table 3 (marked with an asterisk) have close compan-

TABLE 2

LIST OF CONTINUUM SOURCES OBSERVED IN VLA FIELDS[a]

VLA source #	Fields	G.F.	(RA − 8h)	Dec.*	S_{cor} (m Jy)	α
1	b	5.4	$13^m\ 09.5^s$	*57' 58"	5.7	
2	b	4.6	13 16.9	*59 41	10.5	.19
3	b	4.7	13 24.5	02 43	21.8	.74
4	b	2.15	13 30.9	*48 30	2.2	
5	b	1.85	13 38.9	*45 57	4.2	
6	b	2.3	13 40.3	*40 49	13.3	.83
7	a,b	5.1	13 44.4	07 40	61.0	.95
8	b	1.8	13 47.2	*57 34	3.0	
9	b	1.5	13 48.2	*48 29	10.9	.27
10	b	3.8	13 54.4	*32 56	8.6	
11	a,b	1.9	13 55.3	00 23	29.1	.25
12	a,b	2.65	13 59.7	12 46	9.0	
13	a	2.4	14 02.3	14 30	25.1	1.06
14	b	1.8	14 09.6	*37 58	3.4	
15	a,b	1.5	14 19.3	00 46	3.2	1.19
16	b	1.6	14 25.0	*37 49	2.3	
17	b	1.35	14 27.0	*40 16	1.3	
18	a	1.4	14 30.1	19 23	1.4	
19	a	2.1	14 30.5	27 42	10.5	.75
20	b	1.5	14 31.4	01 11	1.3	
21	b	1.0	14 36.4	*47 50	0.8	
23	b	1.0	14 36.9	*51 18	12.2	.15
24	a	1.5	14 37.0	09 43	33.3	.53
25	b	1.2	14 39.6	*38 54	26.8	.71
26	a	1.2	14 40.8	11 25	2.4	
27	a	1.2	14 45.5	19 32	1.2	
28	b	2.7	14 47.4	*32 46	2.8	
29	a,b	1.7	14 48.4	04 26	19.2	.85
30	a	2.0	14 48.8	29 57	1.8	
32	b	2.4	14 49.5	*34 04	15.0	.38
33	a,b,d	1.3	14 51.1	*58 44	9.2	1.00
34	a	3.1	14 51.3	33 35	14.4	.43
35	a,b,d	1.2	14 52.3	*56 50	6.4	
36	d	6.7	14 53.3	*46 37	8.9	
37	a	1.4	14 53.5	25 21	1.0	
38	b	2.4	14 54.3	*34 21	21.8 (94)	−.29
39	a	1.3	14 54.8	07 31	1.3	
40	b	1.1	14 55.9	*50 04	1.2	
41	b	1.2	14 57.3	*55 21	2.0	
42	a	1.0	14 57.4	15 56	0.4	
43	b	6.4	15 01.5	*28 13	8.8	.97
44	a	1.0	15 12.2	14 17	2.0	
45	a,b,d	1.1	15 12.3	09 12	7.1	.75
46	a	1.0	15 15.6	16 16	9.2	.99
47	a,b,d	1.7	15 20.2	02 57	2.6	.56
48	a	1.2	15 25.3	08 30	2.0	
49	d	1.8	15 25.4	*53 40	1.8	
50	d	3.1	15 28.5	07 59	3.5	
51	a	2.7	15 30.2	32 42	2.6	
52	b,d	1.6	15 33.6	*57 37	2.1	
53	d	8.0	15 33.6	*34 29	11.3	
54	a	1.1	15 33.7	13 39	1.2	
55	a,b,d	1.5	15 34.7	*55 06	3.3	.35
56	a	1.1	15 37.0	15 47	0.9	
57	a,c	1.2	15 38.9	19 33	17.2	.68
58	b	3.2	15 39.7	*32 29	9.1	.82
59	a	1.2	15 41.4	12 16	1.6	
60	a,d	1.5	15 41.8	00 37	2.4	.42
61	b,d	1.3	$15^m\ 42.7^s$	*55' 12"	2.7	
62	b,d	2.1	15 44.3	*43 12	3.4	1.06
63	a,c	2.3	15 44.7	30 05	5.5	.72
64	a,d	1.6	15 49.0	07 22	2.0	
65	a	1.5	15 53.8	22 34	1.9	1.01
66	b,d	1.1	16 04.3	*52 20	9.0	.69
67	a,c	1.6	16 06.7	20 36	6.6	.87
68	a,c	1.6	16 07.3	24 30	4.0	.45
69	a,b,d	1.0	16 07.7	*56 12	5.7	.52
70	a,d	1.8	16 08.0	12 37	2.0	.49
71	a,c,d	1.7	16 08.9	15 19	6.9	.72
72	d	1.0	16 10.9	*53 58	5.6	.37
73	d	2.4	16 13.7	*38 57	7.0	
74	a,b,d	1.0	16 14.5	*57 54	5.0	.24
75	d	2.0	16 17.8	*40 12	2.5	
76	d	1.0	16 19.1	*56 35	3.5 (109)	
77	d	2.7	16 23.5	*37 42	3.0	
78	a,c,d	1.5	16 24.9	13 02	3.6	.74
79	d	1.7	16 25.7	*41 59	3.7	
80	d	1.0	16 30.2	*53 26	2.0	
81	d	1.1	16 38.3	*49 45	3.4	.31
82	c,d,f	1.6	16 39.7	06 32	16.7	.64
83	a,c,d	1.1	16 42.7	16 22	31.7	.65
84	d	1.9	16 53.8	*42 44	3.9	.23
85	d	1.5	16 56.9	03 42	2.5	
86	c,d,f	1.7	16 58.8	05 27	4.8	.42
87	c	1.2	17 04.2	13 29	1.3	.97
88	d,f	1.8	17 04.9	*44 48	13.5	.04
89	d	2.6	17 14.1	07 32	3.6	
90	d,f	1.6	17 14.7	*56 44	2.8	.22
91	d	5.2	17 22.7	*38 28	6.0	.44
92	c,e,f	1.2	17 24.2	14 52	27.5	−.19
93	d,f	2.4	17 28.7	*46 54	7.2	.20
94	c,e	1.3	17 33.8	25 40	17.5	.66
95	c,e	1.2	17 34.3	20 18	4.8	.80
96	c,f	1.5	17 42.2	08 52	4.9	.30
97	f	1.3	17 48.1	06 50	6.1	.44
98	d	7.1	17 53.0	05 07	7.1	
99	f	2.9	17 55.2	*42 29	5.1	.70
100	c,e,f	1.9	17 58.8	17 10	86.2	.75
101	c,e,f	1.7	18 00.9	19 15	5.8	.72
102	f	1.2	18 08.8	*51 57	2.6	
103	c,e	1.5	18 11.3	33 11	42.2	.76
104	f	1.1	18 12.2	04 38	1.3	
105	c,e	1.2	18 12.3	26 37	181.3	.78
106	c,e,f	1.3	18 15.9	09 50	26.2	.78
107	c,e,f	1.2	18 21.3	20 12	16.3	−.35
108	c,e,f	1.6	18 26.2	14 50	36.5	.92
109	f	4.7	18 26.7	*39 22	15.4	.43
110	f	1.1	18 27.0	04 05	2.9	
111	c,e,f	1.3	18 27.2	17 26	7.9	.36
112	e	2.4	18 33.6	41 59	24.1	.33
113	c,e	1.0	18 34.9	26 55	21.0	.72
114	f	1.3	18 36.1	*51 52	3.0	.68
115	e	1.0	18 41.8	28 43	1.6	
116	f	1.4	18 43.4	*51 52	3.0	.43
117	e	3.0	18 44.3	43 58	128.4	.82
118	e	1.2	18 45.9	33 23	1.6	
(119)	e,f	1.6	18 46.5	13 31	3.5	0
120	f	1.7	18 51.7	08 47	2.4	.51
121	e	1.5	18 53.9	37 05	4.6	.02

TABLE 2—*Continued*

VLA source #	Fields	G.F.	(RA - 8h)	Dec.*	S_{cor} (m Jy)	α	VLA source #	Fields	G.F.	(RA - 8h)	Dec.	S_{cor} (m Jy)	α
122	h	3.9	18^m 54.1^s	*52' 31"	9.0		183	h,i	1.2	21^m 28.3^s	04' 44"	39.7	.79
123	e,f,h	2.1	18 58.4	10 33	5.1		184	i	4.1	21 30.7	20 05	16.9	
124	e	1.5	19 03.7	15 05	2.6		185	h,i	1.1	21 37.2	06 48	81.0	.46
125	e	1.1	19 05.8	30 30	1.7		(186)	i	9.5	21 43.8	13 24	43.0	
126	e,h	1.2	19 06.4	20 10	5.0	.24	187	i	1.2	21 51.8	34 46	3.7	
127	e	1.5	19 08.0	15 55	2.2		188	g,i	1.1	21 57.0	33 10	4.8	
128	e	2.1	19 09.8	40 26	4.6		189	g,i,j	1.3	21 57.5	28 19	19.5	.45
129	e	2.2	19 16.6	12 02	4.6		190	g,i	1.1	21 58.0	35 30	52.0	.89
130	h	1.5	19 16.7	11 27	3.1		191	i	3.9	22 02.9	55 14	11.9	
131	e,f,h	1.5	19 18.2	10 49	11.7	.47	192	j	3.2	22 12.2	*52 27	8.0	
132	e	2.8	19 22.3	41 38	4.9		193	j	2.6	22 19.5	*54 40	12.0	
133	f,h	1.9	19 26.4	*52 50	5.9	.52						(70)	
134	f,h	1.4	19 31.1	*56 59	57.5	.70	194	i	1.3	22 26.1	26 17	3.7	
135	h	1.1	19 32.0	06 42	3.0	.55	195	i,k	1.8	22 32.2	50 02	6.5	
136	f,h	1.1	19 33.4	03 51	3.2	.79	196	j	2.9	22 38.2	*56 34	11.1	
137	e,g,h	1.6	19 36.4	20 49	4.1		197	j	5.3	22 39.1	*52 00	27.9	.26
138	h	1.1	19 39.4	08 29	3.3		198	j	1.8	22 44.7	06 38	7.1	
139	e,g	4.6	19 39.9	47 00	37.2	.79	199	j	2.2	22 45.0	01 39	19.1	
140	g	9.3	19 40.0	51 33	50.9	.57						(120)	
141	e	4.0	19 40.3	10 13	4.7		200	j	1.8	22 45.3	10 50	7.1	
142	e,g	1.6	19 46.8	35 30	19.0	.79	201	i,k	1.4	22 45.9	45 32	48.0	.45
143	e	1.8	19 47.2	26 37	3.2		202	i,k	1.2	22 55.5	36 18	7.5	
144	g	2.6	19 55.4	45 01	3.1		203	i	3.1	23 15.6	22 05	9.9	
145	g	1.3	19 56.9	27 57	2.3		204	i	3.8	23 18.3	51 00	18.6	
146	h	4.8	19 58.8	*43 50	20.7 (59)	.21	205	i,k	1.6	23 20.8	43 57	5.5	
147	g	1.5	19 59.4	39 13	1.9		206	j	5.7	23 22.1	11 52	24.3	
148	h	1.0	20 02.3	05 49	7.7 (160)		207	k	2.9	23 24.8	55 03	7.4	
							208	i	6.6	23 27.2	18 40	22.6	
149	e,g,h	1.2	20 04.1	27 23	56.2	-.53	209	i,k	1.7	23 34.5	31 00	45.5	
150	g	2.3	20 05.8	45 33	5.1	.79	210	k	1.3	23 35.8	46 14	2.6	
151	h	1.0	20 06.8	05 47	5.4	.62	211	i,k	1.3	23 37.7	36 20	7.0	
152	e,g,h	1.3	20 10.0	14 15	12.0	.64	212	k	2.0	23 38.6	53 38	38.2	
153	h,j	1.1	20 13.6	*59 16	38.0	.76	213	k	1.2	23 41.9	37 29	3.3	
154	h	1.1	20 14.0	01 30	6.7	.02	214	i	4.0	23 48.9	39 32	12.6	
155	e	5.3	20 14.7	18 24	8.9		215	k	1.1	23 54.7	42 03	14.2	
156	j	7.3	20 17.2	00 29	29.1		216	i,k	2.0	23 55.6	26 53	26.6	
157	g	1.4	20 21.6	40 30	1.9		217	k	7.0	24 00.0	18 06	9.5	
158	g	1.2	20 31.1	37 58	6.9	.78	218	k	1.0	24 00.2	43 18	2.9	
159	h	2.5	20 31.8	*49 55	16.5	.82	219	k	1.0	24 08.8	38 45	2.0	
160	h	3.2	20 35.8	*48 25	10.2	.11	220	k	1.2	24 12.9	48 44	4.0	
161	g,h	1.4	20 37.6	10 52	4.0	.75	221	k	2.9	24 19.8	58 40	69.3	
162	g	1.0	20 37.9	30 10	13.0	.05	222	k	2.2	24 21.8	56 35	6.3	
163	h	1.3	20 38.1	04 55	7.5	.15	223	k	1.3	24 25.6	50 09	6.7	
164	g	1.0	20 38.2	28 19	4.7		224	k	1.6	24 34.9	52 03	3.6	
165	g	1.0	20 42.0	30 58	6.6	.11	225	k	3.3	24 44.9	23 52	4.7	
166	g	5.8	20 46.0	52 59	12.3	.71	226	k	1.2	24 47.1	38 44	11.3	
167	g	1.1	20 47.9	25 10	1.8		227	k	1.6	25 00.0	35 27	2.2	
168	g,h,j	1.9	20 49.6	14 30	49.0	.76	228	k	1.6	25 05.6	40 49	4.7	
169	g	1.5	20 53.5	41 57	4.7		229	k	5.4	25 28.6	28 35	12.4	
170	g	1.3	20 55.5	23 30	1.6		230	k	7.3	25 29.4	55 40	13.7	
171	h	6.6	20 58.4	*46 50	426.7	.54	231	k	3.5	25 30.0	46 52	4.6	
172	h	3.6	20 58.5	*51 19	11.7	.32	232	k	5.2	25 38.8	33 40	33.0	
173	g	1.2	20 58.6	24 24	3.0								
174	g	1.3	21 01.1	37 49	1.8								
175	g,h,j	1.4	21 02.0	21 40	16.0	.36							
176	h	2.5	21 03.5	*57 45	4.5								
177	g,j	3.4	21 07.0	48 31	34.0	.74							
178	g,j	1.3	21 07.5	11 37	6.0								
179	j	2.2	21 11.9	*56 55	6.3								
180	g	5.2	21 15.1	11 32	8.2								
181	g	1.7	21 16.6	39 49	2.4								
182	i	5.6	21 22.5	52 31	16.9								

[a]Right ascension for all sources starts with 8^h; the declination starts with 21° unless the numbers in the table are preceded by an asterisk denoting 20°.

ions, one has a faint companion, two (Zw 119080 W and E) form a close pair, and the fourth (Zw 119041) is a close companion to another, undetected, Zwicky galaxy. For the two Zwicky pairs the difference in radial velocities is 145 and 15 km s^{-1}, respectively. The percentage of close companions is larger for the detected than for the undetected galaxies. The mean apparent magnitude for the 16 detected Zwicky galaxies is $\overline{m_p} = 15.2$; there are about 13 undetected galaxies, classified Sa or later, in the same survey area and their mean apparent magnitude is $\overline{m_p} = 15.4$.

For any assumed value of the Hubble constant H_0, we can convert $\overline{m_p}$ into absolute magnitude M_p and flux S_{corr} into total radio power P(W H_z^{-1} at 1.4 GHz). Using the mean group velocities for Cancer A, B, and D and the individual velocities for the three unassigned Zwicky galaxies in Table 3, we plot log P against M_p in Figure 4 for the 16 detected Zwicky galaxies.

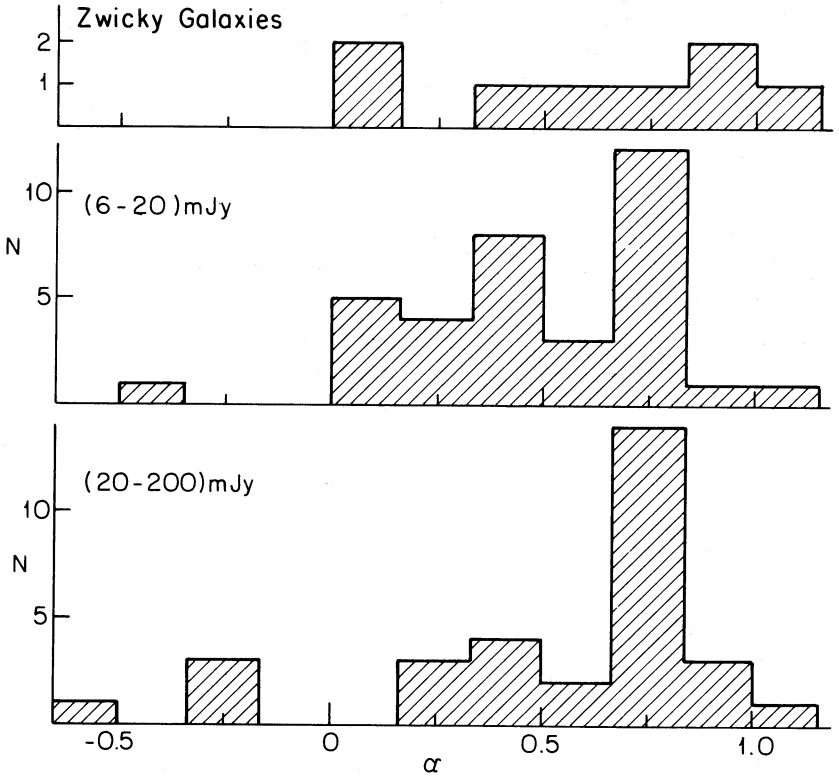

FIG. 3.—The frequency distribution for the spectral index α between 610 MHz and 1.4 GHz for two ranges of (nongalaxy) source fluxes and for the detected Zwicky galaxies.

TABLE 3

RADIO SOURCES IDENTIFIED WITH OPTICAL GALAXIES[a]

VLA Source No.	Zwicky 119 No.	NGC or IC or UGC	Hubble Type	m_p	S_{cor} (mJy)	Optical–Radio R.A. (s)	Optical–Radio Decl. (″)	Group or $V/10^3$ km s^{-1}	S_{60} μm
4	...	...	...	...	2.2	+0.1	−2	...	
14	...	...	...	...	3.4	−0.1	−3	...	
18	28	...	Sa	15.5	1.4	+0.1	−15	2.06	
42	34	...	Ir	15.6	0.4	−0.2	+3	11.14	
55	41	U4324	S?*	15.3	3.3	+0.1	−2	A	0.60
65	43	...	Sa/b	15.5	1.9	+0.2	−4	A	
67	46	U4329	Sc	15.0	6.6	...	...	D	0.56
75	50	N2558	Sb	14.6	2.5	+0.5	−7	A	
78	53	...	S	15.5	3.6	−0.1	−3	A	
83	55	U4332	Pec*	15.5	31.7	+0.1	−2	A	0.86
87	59	...	S	15.7	1.3	−0.3	−1	A	
95	...				4.8	−1.6	+10	...	
110	68	N2570		15.4	2.9	+0.8	+7	B	
125	71	SBa	SBa	15.7	1.7	+0.5	−19	B	
143	...	...	...		3.2	+0.7	−12	...	
162	80W	I2338	Pec*	15.4	13.0	−0.4	−11	A	1.62
165	80E	I2339	Pec*	15.4	6.6	−2.7	−23	A	
178	83	U4386	Sb	14.8	6.0	−0.6	−15	A	0.65
220	103	...	...	15.0	4.0	...	...	7.48	
226	109	N2595	Sc	13.9	11.3	−2.1	−6	A	0.99

[a] An asterisk after the Hubble type denotes the presence of a close companion; V is the recession velocity; S_{60} μm denotes the *IRAS* flux at 60 μm in mJy.

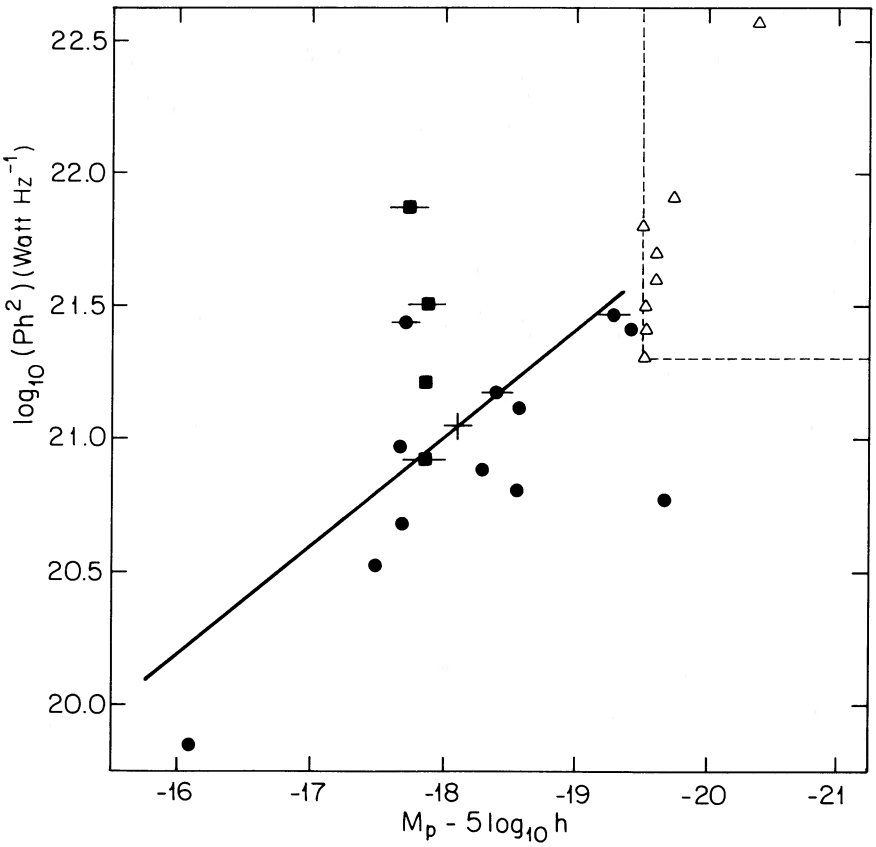

FIG. 4.—Radio power (in WHz) vs. absolute optical magnitude for the Zwicky galaxies in Cancer (*circles*) and a few in Hercules (*triangles*). Distances are computed using $h = H_0/100\,\mathrm{km\,s^{-1}\,mpc^{-1}}$.

The four asterisked galaxies (with a close companion) are denoted by squares, the remaining 12 by circles. The mean values of log P and M_p for the 16 galaxies are shown by a cross in Figure 4 and the straight line through this cross denotes a constant ratio of radio power to optical luminosity. In a previous paper (Dickey and Salpeter 1984) we gave 1.4 GHz fluxes for eight spiral Zwicky galaxies located in the Hercules Cluster (mean velocity $\approx$ 11,000 km s^{-1}). These eight galaxies are also shown in Figure 4 (*open triangles*). Since selection criteria were slightly different in the two surveys, we cannot carry out a quantitative statistical comparison of Cancer and Hercules galaxies. Nevertheless, one qualitative feature stands out quite strongly in Figure 4: Intrinsically very luminous spiral galaxies (which also tend to have a large radio power P) are quite common in the Hercules Cluster, but are absent in the Cancer collection of groups.

Six of the 16 detected Zwicky galaxies in Cancer have a measured *IRAS* flux at 60 μm, given in the last column of Table 3 (also shown by a horizontal bar in Fig. 4). Note that the galaxies with a close companion tend to have large power both at 1.4 GHz and in the 60 μm infrared band. This result fits with the well-documented general positive correlation between radio and 60 μm fluxes (Dickey and Salpeter 1984; de Jong *et al.* 1985; Helou, Soifer, and Rowan-Robinson 1985; Gavazzi, Cocito, and Vettolani 1986).

Of the 16 detected Cancer galaxies nine have measured optical colors (Bothun *et al.* 1985) and seven have measured Hα fluxes (Kennicutt, Bothun, and Schommer 1984). There is quite good linear correlation between the radio flux at 1.4 GHz and the Hα flux, shown in Figure 5. Extrapolating the radio flux up to 90 GHz gives a ratio of 3×10^{-3} for total radio-to-Hα power, almost the same as the ratio found by Kennicutt (1983) for field galaxies. There is little correlation between radio flux and optical color for our Cancer galaxies (if anything, the trend is opposite to that for field galaxies from Kennicutt 1983).

V. THE GALAXYLESS SOURCES

As discussed above, our list of continuum 1.4 GHz sources in Table 2 should be quite reliable above 6 mJy and extremely reliable for a sky flux $S_{cor} \geq 10$ mJy. Of the sources associated with galaxies in Table 3 only three of the Zwicky galaxies (and none of the others) are above 10 mJy. All sources above 10 mJy are mapped in Figure 2 (coded into three flux bins), but for statistical considerations we shall omit the three Zwicky galaxies (each in Cancer A).

As seen in Figure 1, the Zwicky galaxies in our survey area have a concentration (the center of the Cancer A group) in the right-hand half of this area. Figure 2 shows that there is *no* equivalent concentration in the radio continuum sources. Furthermore, we shall show below (Table 4) that the whole right-hand half area has a radio luminosity function which is *not* in excess of the general luminosity function. Thus, very few (if any) of the sources in Figure 2 (except for the Zwicky galaxies) are "galaxyless objects" or faint galaxies in the Cancer Cluster.

Figure 2 provides a complete set of 56 background sources with flux $S_{cor} \geq 10$ mJy over the fairly large survey area of 2.54 deg^2, and we can test for some nonuniformity in the density

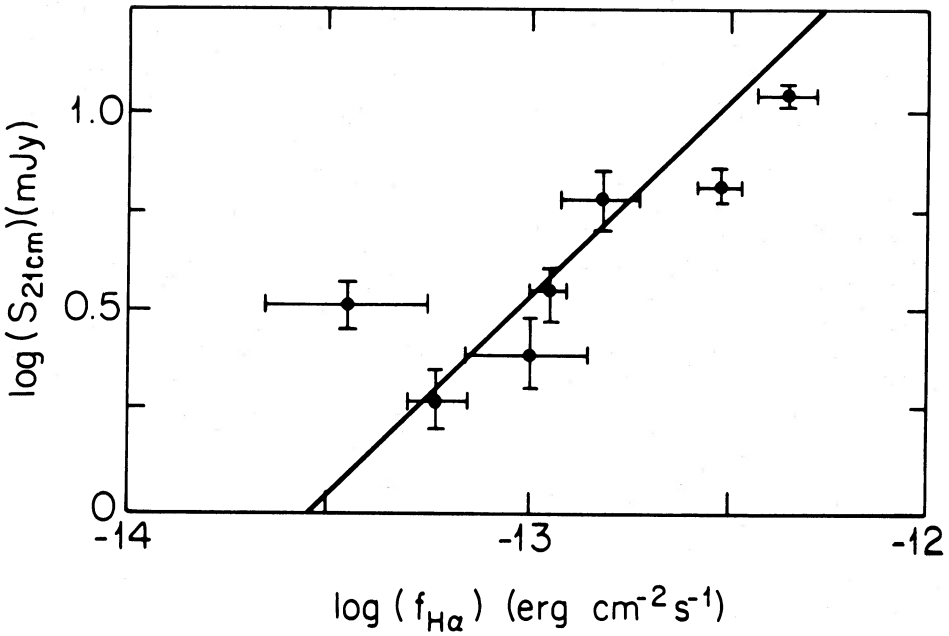

FIG. 5.—The radio flux S at 1.4 GHz plotted against the Hα flux f for the optical galaxies in Cancer. The "best fit" ratio is displayed in the straight line.

distribution. Visual inspection shows that, of the nine strongest sources in the survey area above 50 mJy, most lie toward the left of this area. The solid "line with a kink" in the middle of Figure 2 divides the survey area into two equal halves of 1.27 deg^2 each, in a manner designed to maximize the asymmetry—seven left to two right. Having accentuated the strong-source asymmetry we cannot use it for a quantitative probability assessment (although no other equal-area division could change the sign of the asymmetry). However, we can now test the left/right distribution for other kinds of sources, which is done in Table 4. For the medium-strong sources (20–50 mJy) the asymmetry is still quite strong (14 left to eight right), for the weaker sources (10–20 mJy) the asymmetry is not statistically significant (but still of the same sign). The sources inside the survey area thus suggest a higher source density toward the left than the right (at least for the stronger sources), although not at a good confidence level. However, Table 4 also shows the left/right distribution of sources just outside the survey area, and, in *each* of the three flux bins, there are more sources left than right. This strengthens the suggestion considerably, but makes it likely that correlation lengths for fluctuations in the projected source density tend to be larger than $\sim 1°$.

The average flux distribution for background sources at 1.4 GHz has been given by Oosterbaan (1978) and by Condon and Mitchell (1982). The source counts expected from these compilations are also given in Table 4 for each of three flux ranges. For the right half of the survey area in Figure 2 there are no appreciable discrepancies between the expected and observed counts, even though this is the area containing the core of the Cancer A group. For the left half area, however, the observed counts exceed the expected in each of the three flux bins. The left/right asymmetry is thus likely to be due to a density enhancement on the left rather than a depression on the right.

TABLE 4

OBSERVED AND EXPECTED NUMBERS OF SOURCES[a]

Flux (mJy)	10–20	20–50	>50
Left observed	13	14	7
Left expected	10.8	7.6	3.9
Right observed	12	8	2
Right expected	10.8	7.6	3.9
Left outside	8	5	2
Right outside	2	1	0

[a] In each of three flux ranges, separately for the left and right halves of the survey area. Source numbers just outside the area are also shown (Zwicky galaxies are omitted).

VI. DISCUSSION

a) Optical Galaxies

Our survey area in the Cancer Cluster contains 41 Zwicky galaxies, of which about six are ellipticals and about six are S0 galaxies. None of these 12 early-type galaxies was detected at 1.4 GHz. As mentioned, none of the Cancer cluster galaxies of either early or late type is intrinsically very bright: only one galaxy, the early-type NGC 2563, has $m_p < 14.0$ and the early and late types each have the same mean magnitude of $\overline{m_p} \approx 15.3$. For a nominal value of $H_0 = 100$ km s^{-1} Mpc^{-1}, the absolute magnitudes are in the range $M_p = -(17\text{–}20)$ and the radio continuum detection threshold is of order $10^{20.5}$ W H_z^{-1}. Under these conditions, the general luminosity functions in Figures 2 and 3 of Hummel, Kotanyi, and Ekers (1983) give a detection probability of about 0.2 per E galaxy and about 0.1 per S0. The expected number of detections is then about 1.8. The observed absence of detections is not necessarily discrepant, but the detection probabilities for early-type galaxies in the Cancer Cluster can certainly not be much *larger* than Hummel *et al.*'s average over many locations. An enhanced detection probability has been found for early-type galaxies in a dense environment (Heckman, Carty, and Bothun 1985; Cordey 1986), but only for intrinsically very bright galaxies. The absence of an enhancement in the "giant-less" Cancer Cluster, which is only moderately dense, is thus not surprising.

Of the 41 Zwicky galaxies in our survey area about 29 are

spirals (Sa or later), and only about 13 of these remain undetected at 1.4 GHz. The absolute powers and magnitudes of the 16 detected spirals are plotted in Figure 4 and show a considerable spread in power. Because of this spread it is not clear if the median radio power scales more strongly, or less, than linearly with optical luminosity L for spirals (in contrast with ellipticals where the scaling is appreciably stronger than linear). The 45% undetected spirals have a mean apparent magnitude only 0.2 mag fainter than the 55% detected ones, arguing against a very strong scaling law. Hummel (1981*a*) has derived radio luminosity functions for spiral galaxies from a large sample of bright galaxies, not biased in favor of groups and clusters. He finds our approximately linear scaling law and his Table 2 can be extrapolated to $M_p = -18.0$, the mean absolute magnitude of our 29 spirals for a nominal $H_0 = 100$. This predicts a detection probability of about 40% for powers $P > 10^{20.4}$ W H_z^{-1}, the approximate threshold for our survey. Our observed value of $\sim 55\%$ for the Cancer Cluster is not larger by a significant amount. Our results for four spiral galaxies with a close companion (squares in Fig. 4) corroborates the finding by Dressel (1981) and Hummel (1981*b*) that galaxies with a close companion tend to have enhanced radio continuum emission (and enhanced far-infrared *IRAS* emission). The detected Cancer galaxies also show a positive correlation between radio and Hα flux, i.e., the radio emission from spiral galaxies is associated with other tracers of star-formation activity—at least statistically. Qualitatively the correlation is similar for the Cancer Cluster and for field galaxies, but quantitative results—and the subtler correlations with optical color (Kennicutt 1983) and morphology (Gavazzi, Cocito, and Vettolani 1986)—probably depend on the presence or absence of giant galaxies (absent in Cancer), close pairs (present), etc.

Apart from the 16 Zwicky galaxies in the Cancer Cluster, only four other of our sources coincide with a galaxy on the Palomar survey plate, and each of these has low radio flux and corresponds to a very faint optical apparent magnitude. We cannot tell whether these four cases represent dwarf galaxies in the Cancer Cluster or very distant radio galaxies, but in either case they have little effect on our statistics. Unlike a suggestion for the Hercules Cluster (Dickey and Salpeter 1984), which has intrinsically very bright optical galaxies and head-tail radio sources, we find no evidence for "galaxy-less" sources associated with the core of the Cancer A group (Bothun *et al.* 1983).

b) Background Sources

We have uniform, complete coverage for fluxes above 10 mJy over an area of 2.54 deg^2. The 56 background sources (excluding the 16 Zwicky galaxies) are compatible with the radio luminosity function of Oosterbaan (1978) and Condon and Mitchell (1982), but suggest a nonuniform distribution of source densities per unit solid angle. Having found more sources above 50 mJy in the left half of our survey area than the right (by seven to two), we can look for the distribution for weaker sources (see Fig. 2 and Table 4): For fluxes (20–50) mJy the number in the left exceeded that in the right by 14 to eight, but for (10–20) mJy by only 13 to 12. We thus have a suggestion of a somewhat varying density distribution, at least for the larger fluxes, but not firm evidence. However, we have some corroborating suggestions from two survey fields (~ 9 deg^2 each) obtained by Hazard and his colleagues (Condon, Condon, and Hazard 1982; Coleman, Condon, and Hazard 1985).

We divide their square fields into two equal area rectangles. For field A we find four strong sources (>400 mJy) left to zero right and then compare weaker sources: For (120–400) mJy we find seven left to three right, for (50–120) mJy we have 13 to 10 and for (35–50) mJy we have 14 to 10. The situation is similar for field B with four strong sources (>300 mJy) in the right half area to two in the left: For (100–300) mJy the ratios right to left are 11 to six, for (40–100) mJy we have 20 to 13 and for (25–40) mJy we have only 14 to 13. We thus have the same qualitative picture for these two fields and for our survey area: The asymmetry in source numbers between two half areas is very small for any one flux bin, but (i) the sign of the asymmetry is the same for the different flux bins and (ii) the percentage effects are weaker for weak sources. If these asymmetries of projected number density on scales of one to a few degrees turn out to be real (and not merely statistical fluctuations), they would shed light on nonuniformity of volume density at appreciable redshifts.

Consider first the contribution of the numerous normal galaxies in typical galaxy clusters. Although the density contrast is high in such clusters, the typical radio power of normal galaxies is so low that single clusters with redshift $z \gtrsim 0.04$, say, give a negligible contribution to projected density variations for flux levels $S \gtrsim 3$ mJy (nearer clusters are small in number and well known). Superclusters with sizes (expressing distances in redshift units) of order $\Delta z \sim 0.01$ are still unimportant, but "super-superclusters" might be important with spacings of order $\Delta z \sim 0.1$, as suggested by a number of authors recently (Bahcall and Burgett 1986; Batuski and Burns 1985; DeLapparent, Geller, and Huchra 1986; Tully 1986). As one naive and hypothetical, but concrete, example we start with uniformly populated cubes of length (expressed in redshift units) $\Delta z \sim 0.1$ and then imagine them compressed by various amounts. Let $f(S, z)$ be the fraction of all observed sources with flux S which are at distances between z and $z + 0.1$, for a *uniform* distribution. For the cosmological model and luminosity evolution assumed by Condon and Mitchell (1982), the fraction $f(S)$ for $z \sim 0.5$ is about 0.05 at $S = 10$ mJy and decreases slightly with increasing S. Now assume that each cube is compressed into a "super-supercluster" by some factor F_z along the line of sight, factors F_x and F_y along two mutually perpendicular transverse directions. Assume further that, along a particular line of sight, one cube out of 10 (at $z \sim 0.5$, say) has a particularly strong compression. The enhancement in projected number density is then by a factor of $[1 + (F_x F_y - 1) f(S)]$. For instance, if F_x and F_y are ~ 2 and 4, respectively, then an area of angular size $\sim 5° \times 2.°5$ will have an enhancement at $S \sim 10$ mJy by a factor of about 1.35.

Different combinations of assumed cosmological model and radio-source luminosity evolution can produce the same observed differential source counts and yet predict different forms for the fraction $f(S)$. In particular, models with somewhat less luminosity evolution at the highest radio power levels could give an increasing $f(S)$ with increasing S (above 10 mJy). However, to confirm (or refute) the density inhomogeneities suggested in this paper, uniform surveys over slightly larger areas will be necessary.

This work was supported in part by NSF grant AST 84-15162 to Cornell University and NSF grant AST 82-16879 and NASA grant JPL 957243 to the University of Minnesota. We are indebted to D. T. Keller for help with the optical identifications and to Drs. J. Condon and G. Gavazzi for useful comments.

REFERENCES

Bahcall, N. A., and Burgett, W. S. 1986, *Ap. J. (Letters)*, **300**, L35.
Batuski, D. J., and Burns, J. O. 1985, *Ap. J.*, **299**, 5.
Bothun, G., Aaronson, M., Schommer, B., Mould, J., Huchra, J., and Sullivan, W. 1985, *Ap. J. Suppl.*, **57**, 423.
Bothun, G. D., Geller, M., Beers, T., and Huchra, J. 1983, *Ap. J.*, **268**, 47.
Coleman, P. H., Condon, J. J. and Hazard, C. 1985, *A.J.*, **90**, 1437.
Condon, J. J., Condon, M. A. and Hazard, C. 1982, *A.J.*, **87**, 739.
Condon, J. J., and Mitchell, K. J. 1982, *A.J.*, **87**, 1429.
Cordey, R. A. 1986, *M.N.R.A.S.*, **219**, 575.
DeJong, T., Klien, U., Wielebinski, R., and Wunderlich, E. 1985, *Astr. Ap.*, **147**, L6.
DeLapparent, V., Geller, M. J., and Huchra, J. P. 1986, *Ap. J. (Letters)*, **302**, L1.
Dickey, J. M., Keller, D., Pennington, R., and Salpeter, E. 1987, submitted to *Ap. J.*
Dickey, J. M., and Salpeter, E. E. 1984, *Ap. J.*, **284**, 461.
Dressel, L. L. 1981, *Ap. J.*, **245**, 25.
Gavazzi, G., Cocito, A., and Vettolani, G. 1986, *Ap. J. (Letters)*, **305**, L15.
Giovanelli, R., and Haynes, M. P. 1985, *Ap. J.*, **292**, 404.
Heckman, T. M., Carty, T. J., and Bothun, G. D. 1985, *Ap. J.*, **288**, 122.
Helou, G., Soifer, B. and Rowan-Robinson, M. 1985, *Ap. J. (Letters)*, **298**, L7.
Hummel, E. 1981*a*, *Astr. Ap.*, **93**, 93.
———. 1981*b*, *Astr. Ap.*, **96**, 111.
Hummel, E., Kotanyi, C. G., and Ekers, R. D. 1983, *Astr. Ap.*, **127**, 205.
Kennicutt, R. 1983, *Astr. Ap.*, **120**, 219.
Kennicutt, R., Bothun, G. and Schommer, R. 1984, *A.J.*, **89**, 1279.
Napier, P. and Rots, A. 1982, VLA Test Memorandum No. 134 (Socorro, NM: NRAO).
Oosterbaan, C. E. 1978, *Astr. Ap.*, **69**, 235.
Perola, G. C., Tarenghi, M., and Valentijn, E. A. 1980, *Astr. Ap.*, **84**, 245.
Schommer, R. A., Sullivan, W. T., and Bothun, G. D. 1981, *A.J.*, **86**, 943.
Schuch, N. J. 1983, *M.N.R.A.S.*, **204**, 1245.
Tifft, W., Jewsbury, C., and Sargent, T. 1973, *Ap. J.*, **185**, 115.
Tully, R. B. 1986, *Ap. J.*, **303**, 25.
Valentijn, E. A. 1980, *Astr. Ap.*, **89**, 234.
Zwicky, F. and Herzog, E. 1963, *Catalog of Galaxies and of Clusters of Galaxies*, (Pasadena: California Institute of Technology).

Note Added in Proof.—Recent unpublished Arecibo results by A. J. Phillips make it likely that the sources with the following numbers in Table 2 are spurious: # 36, 155, 182, 184, 186, and 199.

JOHN M. DICKEY: Department of Astronomy, University of Minnesota, Minneapolis, MN 55455

EDWIN E. SALPETER: Center for Radiophysics and Space Research, 424 Space Sciences Building, Cornell University, Ithaca, NY 14853